Published in final edited form as:
J Neurosci Methods. 2014 December 30; 238: 82–87. doi:10.1016/j.jneumeth.2014.09.012.

The use of three-dimensional printing to produce in vitro slice chambers

James Hyde, PhD, **Melanie MacNicol, PhD**, **Angela Odle, PhD**, and **Edgar Garcia-Rill, PhD**
Center for Translational Neuroscience, Department of Neurobiology & Dev. Sci., University of Arkansas for Medical Sciences, Little Rock, AR, USA

Abstract

Background—In recent years, 3D printing technology has become inexpensive and simple enough that any lab can own and use one of these printers.

New Method—We explored the potential use of 3D printers for quickly and easily producing *in vitro* slice chambers for patch clamp electrophysiology. Slice chambers were produced using five available plastics: ABS, PLA, Nylon 618, Nylon 680, and T-glase. These “lab-made” chambers were also made using stereolithography through a professional printing service (Shapeways). This study measured intrinsic membrane properties of neurons in the brain stem pedunculopontine nucleus (PPN) and layer V pyramidal neurons in retrosplenial cortex.

Results—Nylon 680 and T-glase significantly hyperpolarized PPN neurons. ABS increased input resistance, decreased action potential amplitude, and increased firing frequency in pyramidal cortical neurons. To test long term exposure to each plastic, human neuroblastoma SHSY5Y cell cultures were exposed to each plastic for 1 week. ABS decreased cell counts while Nylon 618 and Shapeways plastics eliminated cells. Primary mouse pituitary cultures were also tested for 24-hour exposure. ABS decreased cell counts while Nylon 618 and Shapeways plastics decreased cell counts.

Comparison to Existing Methods—Chambers can be quickly and inexpensively printed in the lab. ABS, PLA, Nylon 680, and T-glase plastics would suffice for many experiments instead of commercially produced slice chambers.

Conclusions—While these technologies are still in their infancy, they represent a powerful addition to the lab environment. With careful selection of print material, slice chambers can be quickly and inexpensively manufactured in the lab.

Corresponding author: E. Garcia-Rill, PhD, GarciarillEdgar@uams.edu, Tel 501-686-5167, Fax 501-526-7928, Director, Center for Translational Neuroscience, University of Arkansas for Medical Sciences, 4301 W. Markham St., Slot 847, Little Rock, AR 72205.

None of the authors have a conflict of interest.

Keywords

3D Printing; PPN; Layer V; thermoplastics

1. Introduction

3D printing as a technology has been around for nearly 30 years, beginning with some of the first attempts by Charles Hull in 1984 (Hull, 1986). In the intervening years, the technology has advanced with many different approaches to producing a physical object from a digital model. Most of these technologies have been controlled by patent restriction. However, these patents are beginning to expire, leading to a new wave of open source 3D printing technologies available to the casual user. This allows basic plastic parts to be quickly produced in the lab for a fraction of the cost normally associated with laboratory supplies. The purpose of this study was to provide a basic introduction to the rapidly advancing field of 3D printing and its potential application to slice electrophysiology.

3D printing is a form of additive manufacture. The physical object is built up from successive layers of material (plastic, metal, etc.). This is opposed to more traditional subtractive manufacturing techniques where material is removed from a block of starting material through cutting, shaping, and grinding. A number of technologies exist for 3D manufacture. Some examples include fused deposition modeling (FDM), selective laser sintering (SLS), and stereolithography. Each method has its own advantages and disadvantages. Currently, only FDM and stereolithography are readily available to the average consumer.

Fused deposition modeling (FDM) is the most basic additive technique. Molten material is extruded through a nozzle head onto a printing bed where it immediately hardens, essentially acting as a hot glue gun. The object is then built up layer by layer to its final form. This is the most common deposition method seen in consumer and do-it-yourself 3D printers. Typically, a thermoplastic such as polylactic acid (PLA) or acrylonitrile butadiene styrene (ABS) is used as the extrusion material. It is fed into the extrusion head as either 1.75 or 3mm diameter plastic filament from a spool. The extrusion material is forced through a nozzle orifice between 200 and 500 μm in diameter and deposited onto the printing platform. One of the major shortcomings of this process is that the printer cannot print extreme overhangs without some variety of support material. Various methods have been devised to solve this problem, but they are beyond the scope of this study. This study will mainly focus on FDM printing.

Other methods of 3D printing include SLS and stereolithography. SLS involves depositing thin layers of plastic, metal, ceramic, or glass powder on the printing surface. A high power laser then selectively fuses the powder to draw a layer of the printed object. A new layer of powder is deposited followed by laser sintering. These steps alternate until the completed object can be removed from the surrounding unsintered powder. Because the surrounding powder provides a support structure, highly complex objects can be printed using SLS, although, this technology is still mainly confined to the realm of industrial manufacturing. Stereolithography uses selective exposure of a light curable photopolymer resin. Each layer

of the printed object is produced by selectively exposing areas of the resin to a scanning laser or a standard computer projector. Consumer versions of this type of printer have only become available in the last two years. One example is the Form 1 printer (Form Labs, Somerville, MA). The advantage of that printing method is that it is one of the most precise printing methods with layers as thin as 25 μm and features as small as 300 μm. The main disadvantage is that the photopolymers are generally toxic and the printed object size is limited due to small build volumes.

We explored 3D printing due to the costs associated with maintaining electrophysiology components such as slice chambers. Some reagents contaminate chambers and can be particularly difficult to remove, e.g. leptin. Thus, we searched for ways to easily and inexpensively make disposable chambers. Components could be made in house using available machining methods, but due to lead time and cost issues we decided to explore consumer 3D printing methods. In order to test the compatibility of 3D printed objects with live cell experiments, we conducted a number of patch clamp and cell culture experiments in the presence of 3D printed thermopolymer plastics and professionally printed photopolymers.

We examined intrinsic membrane and firing properties in neurons of the mesopontine pedunculopontine nucleus (PPN) and pyramidal neurons in retrosplenial cortical layer V. The PPN is mainly involved in waking and paradoxical sleep (Steriade, 1990). As part of the reticular activating system (RAS), the PPN modulates ascending projections to the thalamus as well as descending projections through the pons and medulla. The nucleus is composed of populations of glutamatergic, cholinergic, and GABAergic neurons (Wang and Morales, 2009). Retrosplenial cortex is generally associated with memory and projects to the hippocampal formation (Wyss and Van Groen, 1992).

2. Methods

2.1. 3D Printing

All parts were printed on a Revolution XL printer (QU-BD, Little Rock, AR) equipped with a heated printing bed at 90°C. The extruder was equipped with a 400 μm nozzle using 1.75 mm plastic filament. Exact printing temperatures can be found in the supplementary materials. The printing bed is made of 3/8 inch thick basalt (a volcanic glass) to prevent sagging or warping when heated. Natural color free ABS (acrylonitrile butadiene styrene) and PLA (polyactic acid) plastic filament was from ProtoParadigm (Hermiston, OR). Nylon 618, 680, and T-glase (polyethylene terephthalate polymer) were provided by Taulman3D (St. Louis, MO). Chambers were also printed using the online Shapeways (New York, NY) printing service using the transparent detail plastic, which is an acrylic photopolymer. This plastic was selected due to its being watertight. The control chamber was a RC-26 polycarbonate chamber from Warner Instruments (Hamden, CT).

All parts were designed using Inventor 2014 software (Autodesk, San Rafael, CA). Slice chambers for patch clamp experiments were designed to fit the P-1 Series 20 chamber platform from Warner Instruments. The chamber uses a coverslip bottom to allow for transmitted IR illumination while recording from cells (Figure 1A). Sample disks were

printed from each available media. Each disk was 10 mm wide by 2 mm tall. Each printed object had an individual layer height of 0.1 mm. Files were exported from inventor in the STL format and were imported into the open source G-code generator, Slic3r (Ranellucci, 2014). G-code from Slic3r was then interpreted by the printer control software, Repetier-Host (Hot-World GmbH & Co. KG, Willich, Germany). The control software interfaced with the Azteeg X3 controller on the printer using repetier firmware. A thin coat of ABS 'glue' was applied to the printing bed to ABS, PLA, Nylon 618, and Nylon 680 for better filament adhesion. The glue was later removed with acetone. The glue was made by dissolving ABS filament in acetone until it reached a thick consistency. T-glase adhered to the printing bed without assistance. Small objects (less than a 1cm × 1cm footprint) printed in Nylon tended to detach from the platform even with ABS glue, so that the G-code settings in Slic3r were altered to include a 5 mm skirt on the first printing layer to increase the object's surface area. The skirt was later removed with a scalpel prior to use. We should note that 3D printing community as devised other bed options for working with difficult plastics such as Nylon. These include using wood printing beds or covering a glass/metal bed with standard blue painters tape. However, we found the addition of a skirt in conjunction with ABS glue was sufficient for working with nylon on our printer.

2.2. Electrophysiology

2.2.1. Slice Preparation—All experimental protocols were approved by the Institutional Animal Care and Use Committee of the University of Arkansas for Medical Sciences and were in agreement with the National Institutes of Health guidelines for the care and use of laboratory animals. Rat pups aged 8–16 days were taken from adult timed-pregnant Sprague-Dawley dams. Pups were anesthetized with ketamine (70 mg/kg, i.m.) until the tail pinch reflex was absent. Pups were decapitated and the brain was rapidly removed and cooled in oxygenated sucrose-artificial cerebrospinal fluid (sucrose-aCSF). The sucrose-aCSF consisted of (in mM): sucrose, 233.7; $NaHCO_3$, 26; KCl, 3; $MgCl_2$, 8; $CaCl_2$, 0.5; glucose, 20; ascorbic acid, 0.4; and sodium pyruvate, 2. Sagittal sections (400 μm) containing the PPN nucleus were cut under cooled oxygenated sucrose-aCSF with a Leica VT1200 vibratome (Leica Biosystems, Buffalo Grove, IL) with a Huber mini-chiller (Huber, Offenburg, Germany), and allowed to equilibrate in normal aCSF at room temperature for 1 hr. The aCSF was composed of (in mM): NaCl, 117; KCl, 4.7; $MgCl_2$, 1.2; $CaCl_2$, 2.5; NaH_2PO_4, 1.2; $NaHCO_3$, 24.9; and glucose, 11.5. Slices were recorded at 37°C while being superfused (1.5 mL/min) with oxygenated (95% O_2 and 5% CO_2) aCSF in an immersion chamber. Slices were allowed to equilibrate for 30 minutes in each plastic chamber before recording.

2.2.2. Whole-cell patch-clamp recordings—Infrared differential interference contrast optics was used to visualize neurons using an upright microscope (Nikon FN-1, Nikon, USA) and QICAM camera (QImaging, Surrey, BC). A 40X, 0.8 numerical aperture (NA) fluorite water immersion objective (Nikon) was used. Whole-cell recordings were performed using borosilicate glass capillaries pulled on a P-97 puller (Sutter Instrument Company, Novato, CA), and filled with intracellular solution, designed to mimic the intracellular electrolyte concentration, composed of (in mM) K-gluconate, 124; HEPES, 40; EGTA, 0.2; Mg-ATP, 4; GTP, 0.4 mM; phosphocreatine, 10; and $MgCl_2$, 2. Osmolarity was adjusted to

~270–290 mOsm and pH to 7.3. The pipette resistance was 3–5 MΩ. All recordings were made using a Multiclamp 700B amplifier (Molecular Devices, Sunnyvale, CA, USA) in current clamp mode. Series resistance and liquid junction potential were compensated for. The average series resistance in voltage clamp configuration was 12±0.3 MΩ prior to compensation (>14 KHz correction bandwidth; equivalent to <10 msec Lag.). Average bridge values in current clamp configuration were 13±0.2 MΩ. Analog signals were low-pass filtered at 2 kHz, and digitized at 10 kHz using the Digidata-1440A interface and pClamp10 software (Molecular Devices). Holding current of <− 80pA was used to maintain resting membrane potential of −50mV if necessary.

The recording regions were located mainly in the *pars compacta* in the posterior PPN, immediately dorsal to the superior cerebellar peduncle, and in layer V pyramidal cells in retrosplenial cortex. Gigaseal and further access to the intracellular neuronal compartment were achieved in voltage clamp mode, with the holding potential set at −50 mV. The following intrinsic membrane properties were characterized: resting membrane potential, membrane capacitance, input resistance, action potential (AP) amplitude, and AP frequency. AP amplitudes were determined as averages of 4 APs distributed across a 6 second, 150 pA depolarizing step (Figure 1B). IV curves were generated by 250 msec current pulses from −250 mA to 250 pA in 40 pA steps.

2.3. Cell culture and disc exposure

Human neuroblastoma SH-SY5Y cells (ATCC) were maintained in 1:1 Dulbecco's Modified Eagle's medium: F12 (D-MEM; Life Technologies, Carlsbad, CA) supplemented with 10% FBS (Life Technologies) at 37°C, 5% CO_2 in a humidified atmosphere. 1cm × 2 mm sample discs of each plastic were printed. Discs were "glued" into each well of a sterile 24-well polystyrene tissue-culture-treated dish (Falcon, San Jose, CA) by briefly dissolving the polystyrene surface with acetone and applying pressure (Figure 2A). A drop of acetone was applied to control wells and allowed to dry. The dish containing discs was re-sterilized through 1 hr immersion in 70% ethanol and overnight exposure to UV radiation within the tissue culture bio-cabinet hood. The cells were added to the dish at low density (10^5 cells/ml) and cultured as above with dead cells removed and media changed every three days. Cells remaining after 1 week were removed from the dish through trypsin treatment (0.025% Life Technologies) and live cells were visualized with trypan blue vital stain (Life Technologies) and counted with an average of four counts for each plastic-containing or control well. Cell counts are shown as a percent of the acetone control cell counts. All plastics were tested in at least two separate experiments.

Mouse pituitary cells were acquired from three adult FVB/NJ male mice. The mice were deeply anesthetized using isoflurane and decapitated so that pituitaries could be removed. The three pituitaries were pooled and dispersed using a modified version of a technique previously described (Childs et al., 2011). Briefly, pituitaries were gently dissociated in D-MEM using a TB syringe and 3mg/mL trypsin (Sigma, St. Louis, MO). Following the trypsinization step, pituitaries were dispersed thoroughly in trypsin-free medium and re-suspended in D-MEM fortified with an insulin, transferrin, and sodium-selenite solution (ITS, Sigma, I1884). The cells were then evenly divided among the wells of three 24-well

polystyrene trays containing the different plastics tested (or control wells, exposed to acetone). The trays were incubated at 37°C for 24 hours with gentle shaking to keep the cells in suspension.

On the second day of the experiment, the trays were removed from incubation. The cell-containing media samples were collected from each well, centrifuged, and re-suspended in a small amount of DMEM to concentrate the cells for counting. Samples were counted using a hemocytometer, yielding an average of four counts for each plastic-containing or control well. Cell counts are shown as a percent of the acetone control cell counts.

2.4. Data Analysis

Off-line analyses were performed using Clampfit software (Molecular Devices). Comparisons between groups were carried out using one way ANOVA with Tukey post hoc testing using OriginPro. IV curves were compared with ANCOVA tests in Graphpad Prism (Graph Pad, La Jolla, CA). Note that ANCOVA tests if the regression line slopes are identical, thus, $p \leq 0.05$ indicates that the slopes are identical. All data were tested for normality using the D'Agostino-Pearson omnibus test and was normally distributed ($p \geq 0.05$). Differences were considered significant at values of $p \leq 0.05$. All results are presented as means ± SE.

3. Results

Whole cell patch experiments were performed on a total of 139 neurons, 70 PPN neurons and 67 pyramidal neurons. All PPN neurons were localized as previously described (Garcia-Rill et al., 2007; Garcia-Rill et al., 2008; Simon et al., 2010). Intrinsic membrane properties and IV curves were derived from current pulses (Table 1). IV curves for both PPN and cortical neurons showed no difference between plastics and control (PPN, $F=4.29$ $p=0.0003$; cortex, $F=22.7$ $p<0.0001$). *See* supplementary materials *for IV curves.* Resting membrane potential of PPN neurons showed a number of significant differences (ANOVA $F_{6,59}=6.26$, $p=3.9\times10^{-5}$). PPN neurons exposed to Nylon 680 and T-glase were hyperpolarized in comparison to controls (Nylon 680 vs control, $p=1.02\times10^{-4}$; T-glase vs control, $p=0.003$). Pyramidal neurons showed no difference from control resting membrane potential ($F_{6,60}=1.34$; $p=0.25$). Input resistance showed no difference in PPN neurons (PPN $F_{6,59}=0.96$; $p=0.46$) Cortical neurons exposed to ABS had slightly higher input resistance (ABS vs control, $p=0.05$). Membrane capacitance showed no differences in either cell type (PPN $F_{6,59}=2.16$, $p=0.06$; Cortex $F_{6,60}=1.97$, $p=0.08$). APs showed no difference in amplitude in PPN neurons ($F_{6,58}=1.53$, $p=0.18$). However, ABS exposure decreased AP amplitude in pyramidal neurons (ABS vs control, $p=0.03$). Finally, plastic exposure did not have an effect on PPN neuron AP firing frequency ($F_{6,58}=0.99$, $p=0.44$). ABS cortical neurons showed a significant increase in firing frequency (ABS vs control, $p=0.008$).

Human neuroblastoma SH-SY5Y cells attached to the bottom of each well in culture experiments. Control cells (with acetone treatment but no disk) showed two morphologies, flat, adherent with neurites and rounded, anchorage-independent (Figure 2B) (Ross et al., 1983). Exposure to Nylon 680 and T-glase plastics did not affect cell growth or morphology. However, significantly decreased cell counts were observed when cells were exposed for

long term (1 week) to Nylon 618 or to Shapeways plastics, with Shapeways plastics being particularly toxic to the cells. ABS was also somewhat toxic to cells ($F_{6,42}$=50.29, $p=9.5\times10^{-5}$; ABS vs control, p=0.005; Nylon 618 vs control, $p=1.8\times10^{-4}$; Shapeways vs control, 3.3×10^{-6}: Figure 3).

Pituitary mouse cells were collected and cultured in solution with sample discs of each plastic. Similar to the effect upon neuroblastoma cells, pituitary cells showed significant decreases when exposed to ABS, Nylon 618, and Shapeways plastics ($F_{6,42}$=28.2, $p=3.04\times10^{-13}$; ABS vs control, p=0.03; Nylon 618 vs control, $p=2.46\times10^{-6}$; Shapeways, p=0: Figure 4). Nylon 680 and T-glase were not toxic to pituitary cells. See supplementary materials for cell counts.

4. Discussion

The purpose of these studies was to determine the feasibility of utilizing patch clamp slice chambers fabricated using generally available 3D printer technology. We tested a variety of the available 3D printing plastics and their effects on neurons. Each type of plastic presented challenges when used in a FDM printer. All of the plastics worked well for making simple slice chambers equipped for continuous ACSF flow and a coverslip floor for microscope visualization. ABS and PLA plastics are generally the easiest to work with, as most of the current printers available are designed to use these plastics. Nylon 680 and Nylon 618 produce very clean prints, although, we had extensive difficulty keeping the print attached to the printer stage due to Nylon's slipperiness. Thus, a combination of ABS glue and a skirt of plastic on the first print layer overcame this problem. T-glase has excellent stage adhesion properties, as it was also designed specifically for FDM printers. T-glase does, however, produce strings as the extruder moves from one area of the part to another. These can be easily cut off later using a scalpel. The Shapeways detail plastic was selected due to its watertight properties. Unfortunately, the photopolymers used appeared to be highly toxic for long-term studies.

Patch clamp studies showed that short term exposure (<1 hr) did not greatly affect most intrinsic membrane properties. Interestingly, T-glase and Nylon 680 significantly hyperpolarized PPN neurons. This may be because compounds in either of these plastics activate some variety of potassium channels or alter other channel conductances (Asano et al., 2010; Rottgen et al., 2014; Wang et al., 2011). This may also be because the cells are healthier in the presence of these two plastics. Nylon 680 is a pure nylon polymer that lacks the additives used in other types of Nylon such as 618. T-glase, as a variety of PETT (polyethylene terephthalate) plastic in the polyester family, is most similar extruded plastic in appearance to the polycarbonate plastics normally used in patch clamp or cell culture chambers. The shapeways chambers looked nearly identical to the control chambers. ABS showed the most significant effect on cortical pyramidal neurons and caused an increased input resistance and correspondingly decreased AP amplitude. ABS also increased AP firing frequencies. These effects could be due to compounds in the ABS plastic, which may block ion channels or change channel kinetics, leading to increased firing frequency. These differences were not observed in PPN neurons, which comprise a heterogeneous population with six categories of thalamic projecting neurons as distinguished by *in vivo* recordings of

their firing properties relative to ponto-geniculo-occipital (PGO) wave generation (Steriade et al., 1990). Some sub types exhibit low rates of firing (<10 Hz) while the majority had higher firing rates (20–80 Hz). The PPN has non-overlapping populations of cholinergic, glutamatergic, and GABAergic neurons (Wang and Morales, 2009). The combination of distinct cells types may mask effects upon a particular cell type.

While the patch clamp experiments indicated the few effects of short term plastic exposure, we were also interested in the effects of long term exposure. In order to identify these effects, we used two different cell culture models. The first model used human neuroblastomoa SH-SY5Y cells exposed to each plastic for one week. The space in the culture well around the plastic disc allowed for inspection of the cells. Consistent with the findings from the patch clamp experiments, the cells were healthy in the presence of either Nylon 680 or T-glase. Nylon 618, in contrast, resulted in extensive loss of cells indicating that the cells are particularly sensitive to differences between the two Nylons. The Nylon 618 toxicity may be due to the known property of nylon to produce traces of hydrogen cyanide when heated (Bott, 1969). The Shapeways plastic also caused cell death in long term studies, perhaps due to the photopolymers, which are known to be toxic. We also utilized a medium-term model of mouse pituitary neurons in primary cell culture exposed to each plastic for 24 hours. The results mirrored those seen in the long term neuroblastoma cell model. Nylon 618 and Shapeways exposure resulted in significantly decreased cell counts. ABS also caused a significant decrease in cell counts in this model. Interestingly, ABS showed a significant decrease while PLA did not. This may be because ABS affects pituitary cells differently from neuroblastoma cells, or because a longer exposure time is necessary for PLA to break down the cells.

We conclude that different plastics have differing effects depending on the timeline of the experiments. Obviously, Nylon 618 and Shapeways detail plastics should be avoided due to their toxic effects in medium or long-term cultures. However, ABS, PLA, Nylon 680, and T-glase plastics would suffice for many experiments. The choice between them depends on the type of structures to be printed, as each plastic has different structural qualities as well as ease of use. Ease of use in turn depends on the type of printer used. Most printers currently available are geared to work mainly with PLA and/or ABS plastic. ABS can have stronger structural qualities than PLA. T-glase showed excellent general qualities and is closest to plastics normally used in electrophysiology chambers and cell culture dishes, but is more difficult to work with. The field of consumer level 3D printing is rapidly advancing and has only been readily available for a few years. We will soon see a variety of new plastics available with greatly increased printing resolution and speed. Finally, we anticipate that new advances in printing technology will make 3D printing even easier for lab use, resulting in less focus on how to produce a component and more emphasis on what components should be produced with a simple and rapid production time.

Supplementary Material

Refer to Web version on PubMed Central for supplementary material.

Acknowledgments

Work was performed at the University of Arkansas for Medical Sciences, Little Rock, AR, USA. This work was supported by USPHS award R01 NS020246, and by core facilities of the Center for Translational Neuroscience supported by P20 GM104325 and P30 GM110702 (to EGR) and UL1 TR000039.

The authors would like to thank Qu-BD for their assistance with use of the 3D printer as well as supplying ABS and PLA filaments. We would also like to thank Thomas Taulman of Taulman3D for providing Nylon 618, 680, and T-glase filaments.

References

Asano S, Tune JD, Dick GM. Bisphenol A activates Maxi-K (K(Ca)1. 1) channels in coronary smooth muscle. British journal of pharmacology. 2010; 160:160–70. [PubMed: 20331605]

B, Bott JGF, Jones TA. Evolution of toxic gases from heated plastics. British Polymer Journal. 1969; 1:203–4.

Childs GV, Akhter N, Haney A, Syed M, Odle A, Cozart M, Brodrick Z, Gaddy D, Suva LJ, Akel N, Crane C, Benes H, Charlesworth A, Luque R, Chua S, Kineman RD. The somatotrope as a metabolic sensor: deletion of leptin receptors causes obesity. Endocrinology. 2011; 152:69–81. [PubMed: 21084451]

Garcia-Rill E, Heister DS, Ye M, Charlesworth A, Hayar A. Electrical coupling: novel mechanism for sleep-wake control. Sleep. 2007; 30:1405–14. [PubMed: 18041475]

Garcia-Rill E, Ye M, Heister D. Novel Mechanism for Sleep-Wake Control: Electrical Coupling. SRS bulletin. 2008; 14:8–10. [PubMed: 23125968]

Hull CW. Apparatus for production of three-dimensional objects by stereolithography. Google Patents. 1986

Ranellucci A. Slic3r. 2014 open source.

Ross RA, Spengler BA, Biedler JL. Coordinate morphological and biochemical interconversion of human neuroblastoma cells. Journal of the National Cancer Institute. 1983; 71:741–7. [PubMed: 6137586]

Rottgen TS, Fancher IS, Asano S, Widlanski TS, Dick GM. Bisphenol A activates BK channels through effects on alpha and beta1 subunits. Channels. 2014:8.

Simon C, Kezunovic N, Ye M, Hyde J, Hayar A, Williams DK, Garcia-Rill E. Gamma band unit activity and population responses in the pedunculopontine nucleus. Journal of neurophysiology. 2010; 104:463–74. [PubMed: 20463196]

Steriade, M.; McCarley, RW. Brainstem Control of Wakefulness and Sleep. Plenum; New York: 1990.

Steriade M, Pare D, Datta S, Oakson G, Curro Dossi R. Different cellular types in mesopontine cholinergic nuclei related to ponto-geniculo-occipital waves. The Journal of neuroscience: the official journal of the Society for Neuroscience. 1990; 10:2560–79. [PubMed: 2201752]

Wang HL, Morales M. Pedunculopontine and laterodorsal tegmental nuclei contain distinct populations of cholinergic, glutamatergic and GABAergic neurons in the rat. The European journal of neuroscience. 2009; 29:340–58. [PubMed: 19200238]

Wang Q, Cao J, Zhu Q, Luan C, Chen X, Yi X, Ding H, Chen J, Cheng J, Xiao H. Inhibition of voltage-gated sodium channels by bisphenol A in mouse dorsal root ganglion neurons. Brain research. 2011; 1378:1–8. [PubMed: 21241682]

Wyss JM, Van Groen T. Connections between the retrosplenial cortex and the hippocampal formation in the rat: a review. Hippocampus. 1992; 2:1–11. [PubMed: 1308170]

Highlights

We tested a variety of 3D printed plastics for chambers for patch clamp and cell culture.

Nylon 618 and Shapeways detail plastics were toxic to cells in culture.

ABS, PLA, T-Glase and Nylon 680 can be used depending on the length of exposure.

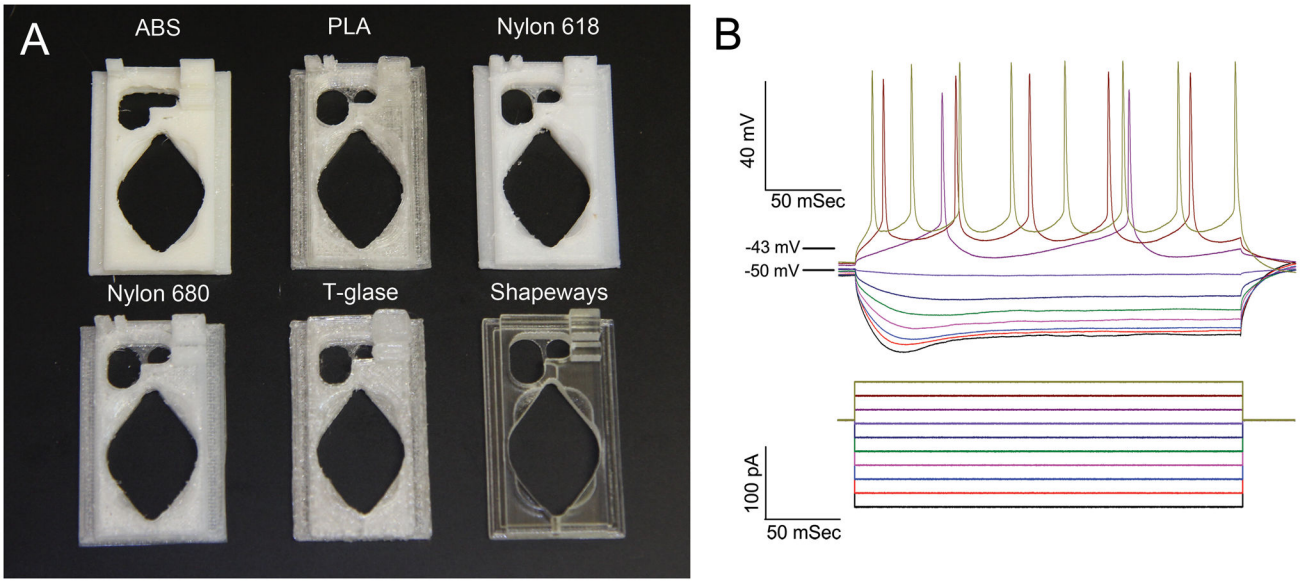

Figure 1. A. Examples of printed chambers in each plastic. B. Representative series of depolarizing steps and APs from a patched PPN neuron

Cells were held at −50 mV with 250ms current pulses from −250 pA to 250 pA. APs occurred between on average at −43±0.6mV in PPN neurons and −45±2mV in cortical neurons.

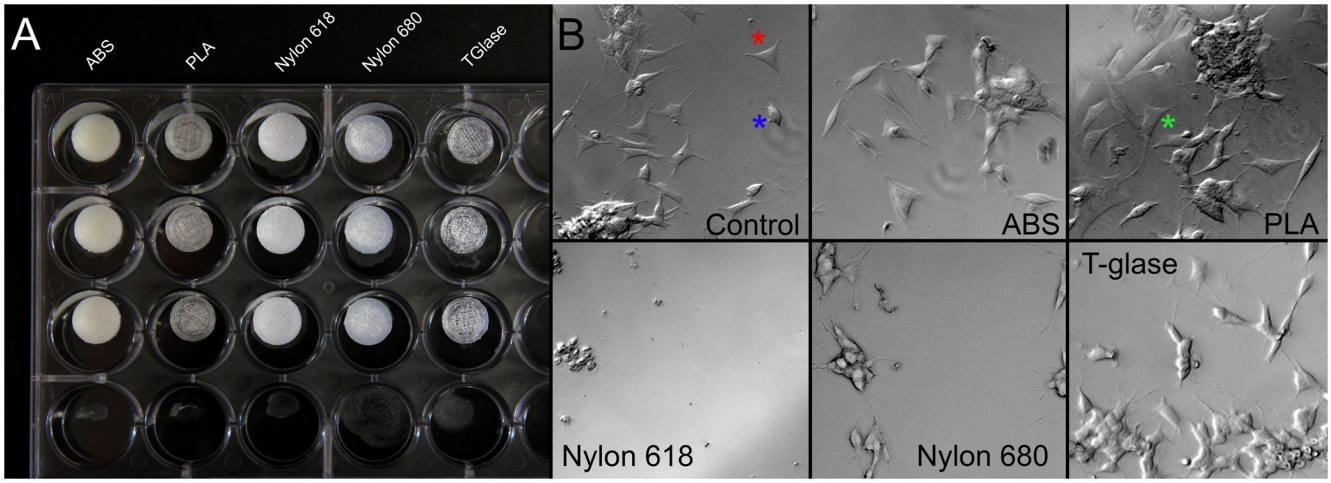

Figure 2.

A. **1 cm sample disks of each plastic**. Shapeways disks were not photographed. B. **Human neuroblastoma cells attached to the bottom of each culture dish well.** The acetone created grooves in the plastic, to which cells adhered. Control cells (with acetone treatment but no disk) showed two morphologies, flat, adherent with neurites (red star) and rounded, anchorage-independent (blue star). Exposure to ABS, Nylon 680 and T-glase plastics did not have obvious effects upon cell growth or morphology. Nylon 618 resulted in an extensive loss of cells and PLA resulted in an exaggerated anchorage-independent morphology (green star). Shapeways killed all cells and thus is not shown.

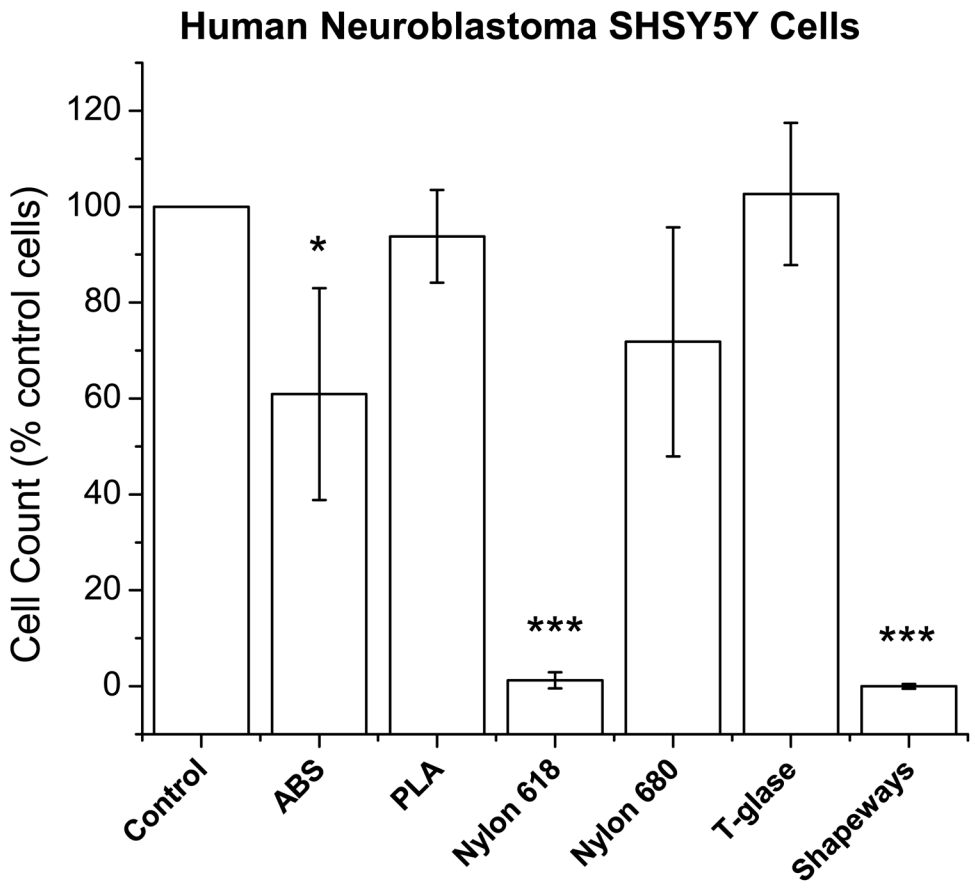

Figure 3. Cell counts of human neuroblastoma cells presented as percent of the control cells (with acetone treatment)

ABS, Nylon 618, and Shapeways plastics showed a significant decrease in cell counts. Note, only significance between plastic and control is marked. Error bars are ± SE. *P<0.05; **P<0.01; ***P<0.001.

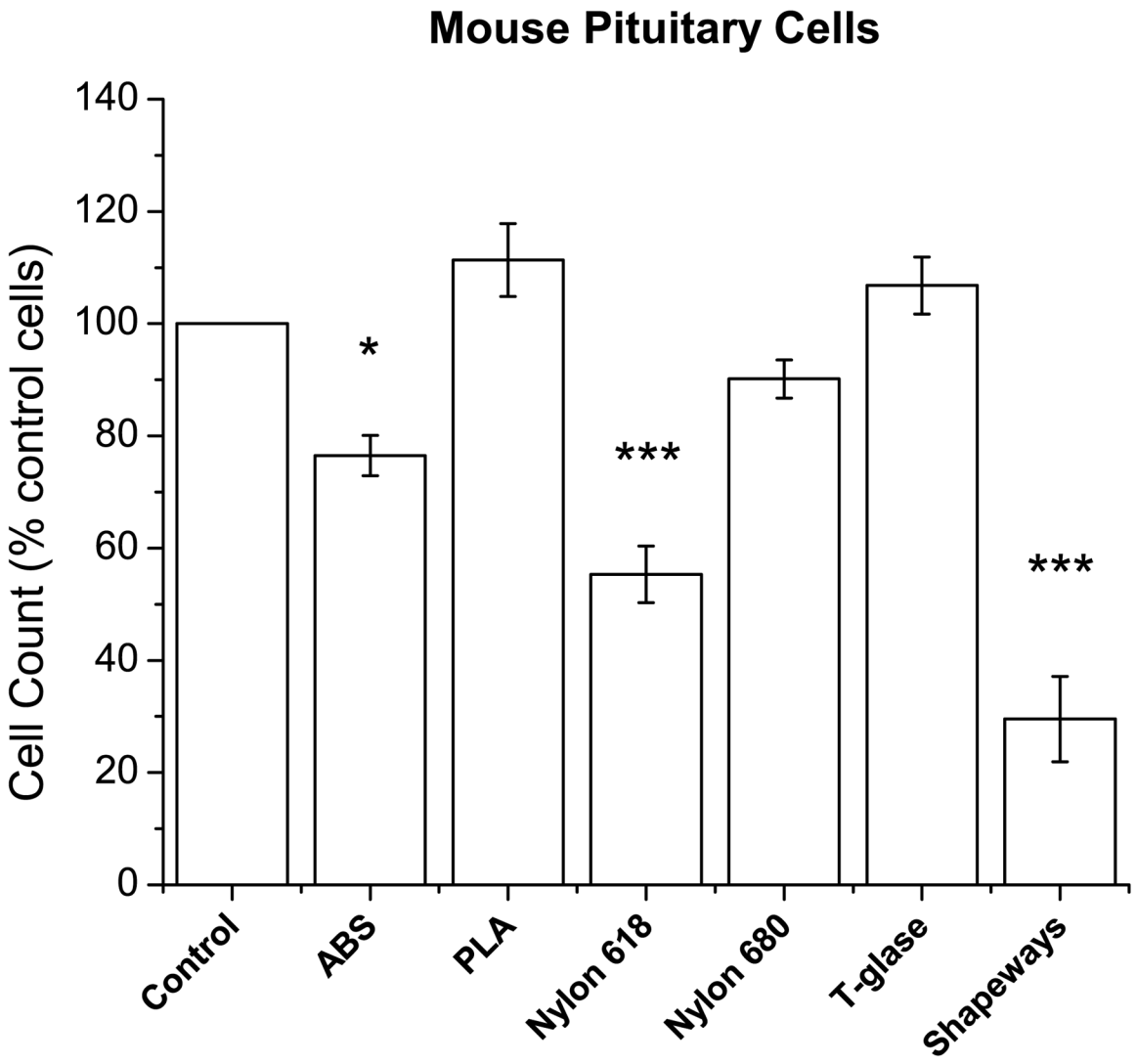

Figure 4. Cell counts of mouse pituitary neurons presented as percent of the control cells (with acetone treatment)

ABS, Nylon 618, and Shapeways plastics showed a significant decrease in cell counts. Note, only significance between plastic and control is marked. Error bars are ± SE. *P<0.05; **P<0.01; ***P<0.001.

Table 1

Intrinsic membrane properties of PPN neurons and layer V cortical pyramidal neurons in the presence of each plastic.

PPN Neurons					
	Resting Membrane Potential (mV)	**Input Resistance (MOhm)**	**Membrane Capacticance (pF)**	**AP Amplitude (mV)**	**AP Frequency (Hz)**
Control n=13	−51±1	364±33	25±2	(n=14) 54±2	23±3
ABS n = 7	−51±2	330±41	25±3	55±4	30±3
PLA n = 9	−56±3	350±39	36±4	(n=8) 63±5	31±7
Nylon 618 n = 8	−58±3	391±31	32±3	55±4	16±3
Nylon 680 n = 10	−66±2***	420±24	28±2	(n=9) 56±4	26±6
T-glase n = 8	−64±2**	409±25	34±4	65±5	24±6
Shapeways n = 11	−55±1	380±16	28±2	62±3	22±4
	F(6,59) =6.26, p = 3.9×10^−5	F(6,59) = .096, p = 0.46	F(6, 59) = 2.16, p = 0.06	F(6,58) = 1.53, p = 0.18	F(6, 58) = 0.99, p = 0.44

LV Cortical Pyramidal Neurons					
	Resting Membrane Potential (mV)	**Input Resistance (MOhm)**	**Membrane Capacticance (pF)**	**AP Amplitude (mV)**	**AP Frequency (Hz)**
Control n=10	−66±1	335±10	92±11	71±4	11±2
ABS n = 10	−69±1	392±10*	69±12	(n=8) 56±3*	25±5**
PLA n = 8	−69±4	316±14	101±9	72±3	16±2
Nylon 618 n = 8	−66±1	358±7	100±6	73±4	17±3
Nylon 680 n = 10	−67±1	328±17	92±4	78±3	15±2
T-glase n = 10	−69±1	356±13	84±6	67±3	16±6
Shapeways n = 11	−63±3	353±17	95±4	(n=10) 69±3	15±4
	F(6,60) = 1.34, p = 0.25	F(6,60) = 3.36, p = 0.006	F(6,60) = 1.97, p = 0.08	F(6,57) = 4.01, p = 0.002	F(6,57) = 2.49, p = 0.03

Note, only significance between plastic and control is marked.

* P<0.05;

** P<0.01;

*** P<0.001.